Journal of Pest Science
https://doi.org/10.1007/s10340-024-01826-6

ORIGINAL PAPER

Physalis floridana suppresses the expression of trehalase gene *HvTREs* in *Henosepilachna vigintioctopunctata* (Coleoptera: Coccinellidae) for defense against herbivorous insects

Xian-Zhong Wang[1,2] · Si-Jing Wan[1] · Bin-Er He[1] · Shuang-Le Wang[1] · Tian-Wen Wang[1] · Liu-He Yu[1] · Shi-Gui Wang[1] · Hui-Zhong Wang[1,2] · Bin Tang[1] · Jiang-Jie Lu[1,2]

Received: 17 April 2024 / Revised: 13 July 2024 / Accepted: 5 August 2024

Abstract

Plants use various secondary chemicals in their chemical defense against herbivores. While botanical insecticides are crucial for reducing the reliance on chemical pesticides, the development of plant-derived insecticides remains limited. In this study, we fed *Henosepilachna vigintioctopunctata* with three different host plants (*Solanum nigrum*, *Solanum tuberosum*, and *Physalis floridana*) and observed that feeding on *P. floridana* led to changes in the body size and a significantly high mortality rate. Through transcriptome analysis, it was found that the trehalose metabolism pathway of *H. vigintioctopunctata* changed significantly under different host feeding conditions, especially since the expression level of the trehalase gene was extremely different. We subsequently identified eight transcripts of *HvTREs* and analyzed their evolution and structure. Among them, significant differences are observed in the relative expression levels of *HvTRE1-5* in *H. vigintioctopunctata* after the fourth instar and were affected by different plant diets. Compared with the natural host *S. nigrum*, the larvae that fed on *P. floridana* significantly reduced the contents of trehalose, glucose and glycogen and significantly affected the trehalase activity. Knockdown of *HvTRE1-5* by RNAi increased mortality at the *H. vigintioctopunctata* prepupation stage, suggesting that *HvTRE1-5* is important for *H. vigintioctopunctata* pupation. This study provides new insights into developing of green control methods for *H. vigintioctopunctata* and offers a valuable example for understanding the interaction between host plants and herbivorous insects.

Keywords Herbivore · *Henosepilachna vigintioctopunctata* · *Physalis floridana* · Trehalase · RNA interference · Phytopesticides

Communicated by Subba Palli.

✉ Bin Tang
tbzm611@hznu.edu.cn

✉ Jiang-Jie Lu
lujj@hznu.edu.cn

Xian-Zhong Wang
wangxz9264@163.com

Si-Jing Wan
wsjw9898@163.com

Bin-Er He
2021210315068@stu.hznu.edu.cn

Shuang-Le Wang
2021210315186@stu.hznu.edu.cn

Tian-Wen Wang
2021210315289@stu.hznu.edu.cn

Liu-He Yu
2021210315167@stu.hznu.edu.cn

Shi-Gui Wang
sgwang@hznu.edu.cn

Hui-Zhong Wang
whz62@163.com

[1] College of Life and Environmental Sciences, Hangzhou Normal University, Hangzhou 311121, Zhejiang, People's Republic of China

[2] Zhejiang Provincial Key Laboratory for Genetic Improvement and Quality Control of Medicinal Plants, Hangzhou Normal University, Hangzhou 311121, Zhejiang, People's Republic of China

Published online: 10 August 2024

Introduction

Physalis floridana, a representative species of the genus *Physalis*, is an important member of the Solanaceae family (Gong et al. 2021). This genus is rich in steroidal compounds, particularly physalins and withanolides, which have been shown in previous research to possess antibacterial, analgesic, anti-inflammatory, and anticancer activities (Januario et al. 2002; Wu et al. 2004; Qiu et al. 2008; Popova et al. 2020a, b). The researches on the *Physalis* plants have gained increasing attention in the field of phytopharmacology. However, in addition to their medical effect, the steroidal compounds in *Physalis* plants have potential as botanical insecticides. Studies on the insecticidal properties of *Physalis* plants indicate that steroidal compounds exhibit insecticidal activity through two main mechanisms: feeding deterrents and growth inhibitors (Weissenberg et al. 1998; Dyer et al. 2003; Prieto et al. 2007; Sell et al. 2021). One of the characteristic features of *P. floridana*, an annual *Physalis* plant, is the dense trichome covering its stems and leaves (Lu et al. 2021). Trichome serves as a vital defense mechanism in plants, releasing volatile organic compounds (VOCs), exuding repellents, alkaloids, and secondary metabolites to fend off insect pests and pathogens (Murungi et al. 2016; Tissier et al. 2017; Burgueno et al. 2023). Therefore, in the present study, *P. floridana* was used to investigate the insecticidal effect and mechanism.

Henosepilachna vigintioctopunctata is a destructive pest insect belonging to the family *Coccinellidae* in the order Coleoptera. This herbivorous ladybird beetle is a notorious pest of Solanaceae vegetables, posing a significant threat to important crops such as potatoes, tomatoes, and eggplants, as well as causing damage to cucurbitaceae and other horticultural crops (Zhang et al. 2002). It is widely distributed in Southeast Asia and parts of Australia. Currently, the primary method of control is chemical insecticides, but their ecological damage and toxicity residues are widely criticized. Therefore, there is an urgent need for greener and more effective control methods for *H. vigintioctopunctata* (Guo et al. 2023).

In insects, trehalose is not only a crucial source of energy but also plays a significant role in important physiological processes like growth, development, and molting (Tang et al. 2012; Shukla et al. 2015). Trehalase (TRE) is widely present in various eukaryotic organisms, and trehalose, a ubiquitous non-reducing sugar in nature, serves diverse functions in different species, such as providing energy, exerting protective effects, and serving as a signaling molecule (Galand 1989; Wingler 2002; Liu and Jiang 2014; Sakaguchi 2020; Luo et al. 2022). Importantly, numerous studies have highlighted the vital roles of trehalose and trehalase in insects' responses to biotic and abiotic stress (Wang et al. 2017; Tang et al. 2018; Yu et al. 2020; Masoumi et al. 2021; Tellis et al. 2023a, b; Wan et al. 2023a, b).

Plant secondary metabolites commonly play a significant role in resisting herbivorous insects, and leveraging the antagonism between plants and insects for pest control is a long-standing practice. Identifying and developing more plants with insecticidal properties is crucial for the advancement of plant-based pesticides (Ricupero et al. 2022; Verheggen et al. 2022). In this study, we investigated the growth effects on *H. vigintioctopunctata* which was fed with three different Solanaceae plants (*S. nigrum*, *S. tuberosum*, and *P. floridana*). We used transcriptomics to explore potential reasons for the high mortality of *H. vigintioctopunctata* after feeding on *P. floridana*. The results indicate that changes in host plants significantly affect the trehalose metabolism of *H. vigintioctopunctata*, potentially affecting its pupation. These findings provide valuable information and theoretical basis for the development of new phytopesticides to control pests such as *H. vigintioctopunctata*.

Materials and methods

Host plant cultivation

The seeds of *P. floridana* were sourced from our laboratory, while the *S. nigrum* seeds were collected in August 2022 from the campus of Hangzhou Normal University (120°02'E, 30°30'N). Potato (*S. tuberosum*) tubers were obtained from Qingdao Jinmandi Potato Co., Ltd. And the tomato (*S. lycopersicum*) seeds were bought from Qingfeng Seed Industry Co., Ltd. All plants were grown in soil and cultivated in a climate-controlled chamber at 26 ± 1 °C, 70 ± 5% humidity, with a light cycle of 16 L: 8D.

Insect rearing

H. vigintioctopunctata were collected from the leaves of dragon fruit plants at the campus of Hangzhou Normal University in August 2022 (120° 02' E, 30° 30' N) and reared in a controlled environment chamber at 28 ± 1 °C, 60 ± 5% humidity, under a light–dark cycle of 17 L: 7D. Larvae were reared in square plastic containers (the dimensions are 10 cm* 5 cm* 5 cm) with small holes. First and second instar larvae were fed using *S. nigrum* leaves, whereas different host plant leaves were used to feed larvae after the second molt. Enough leaves were placed in plastic containers to feed the larvae. Host plant leaves in plastic containers were replaced every 12 h. Adults were reared in

gauze cages (the dimensions are 50 cm* 50 cm* 60 cm) and fed by two-month-old *S. nigrum* plants.

Grouping and sample collection

Larvae fed *S. nigrum*, *S. tuberosum*, *S. lycopersicum*, and *P. floridana* leaves corresponded to the LK, POT, TOM, and PF groups, respectively. Each group of larvae was sampled 108 h after the second molt for transcriptome sequencing. Each sample consisted of three biological replicates, with each replicate containing three larvae.

Moreover, additional larvae from each group were sampled every 24 h from the completion of the fourth molt until 24 h after pupation. Eight kinds of samples were obtained from each group, each sample containing six biological replicates and each replicate containing three larvae. Three biological replicates were used for qRT-PCR, and the other three biological replicates were used to determine carbohydrate content and trehalase activity.

Appearance observation, and biological assay

At least 15 larvae from each group were used for appearance observation and weighing. Appearance images of all insects were captured using a Leica EZ4 HD Stereo Microscope (Leica, Wetzlar, Germany). Larvae were weighed daily using an analytical balance. The weight gain was obtained by subtracting the body weight on the first day from the body weight on the last day of the corresponding developmental stage. Additionally, 60 larvae from each group were observed daily for mortality.

RNA sequencing and data processing

Collected samples were transported to Beijing Genomics Institute (BGI) using dry ice after freezing in liquid nitrogen. RNA purification, reverse transcription, library construction, and sequencing were conducted at BGI. The sequencing platform used was the BGI Genomics DNBSEQ platform, with initial data filtered using the SOAPnuke software to obtain clean reads (Chen et al. 2018). De novo assembly of clean reads (PCR duplicates removed to enhance assembly efficiency) was performed using Trinity, followed by clustering and redundancy removal of assembled transcripts using TGICL to construct a reference gene library. The clean reads were aligned to the reference gene sequences using Bowtie2 to obtain alignment results. The software Transdecoder, recommended by Trinity, was employed to identify candidate coding regions in Unigene, where the longest open reading frame was initially extracted and then homologous protein sequences were predicted through Blast alignment against SwissProt and Pfam searches using Hmmscan to predict coding regions. The assembled Unigene was annotated in seven major functional databases (KEGG, GO, NR, NT, SwissProt, Pfam, and KOG). Clean reads were aligned to the reference gene library using Bowtie2, followed by RSEM to calculate gene expression levels for each sample. Differential gene expression analysis between groups was conducted using DESeq2, with genes considered differentially expressed when the $P \leq 0.05$ (Anders and Huber 2010).

Phylogenetic analysis

The TRE protein sequence of *H. vigintioctopunctata* was obtained from our transcriptome data by using "trehalase" as a keyword to filter results from the seven major databases mentioned. After identifying the corresponding gene IDs, the coding sequences were translated into protein sequences. The TRE protein sequence for *Harmonia axyridis* was sourced from the NCBI database using the same keyword and species-specific limits to search and download the protein sequence. The TRE protein sequences for *Coccinella septempunctata*, *Propylea japonica*, *Cryptolaemus montrouzieri*, *Tribolium castaneum*, and *Nilaparvata lugens* were retrieved through the same keyword search method from InsectBase 2.0 (Mei et al. 2022). The construction of the phylogenetic tree relies on MEGA11 software (Tamura et al. 2021), with visualization done using the online software iTOL (Letunic and Bork 2007). The construction method was the maximum likelihood method with 500 bootstrapping times.

Prediction for protein subcellular localization and motif analysis

The Subcellular localization of TRE proteins was adapted to the Bologna Unified Subcellular Component Annotator (BUSCA) online tool with all parameters as default (Savojardo et al. 2018).

The sequence source is consistent with the previous section. Motif analysis was conducted online using The MEME Suite software (Bailey et al. 2009). The site distribution was set as Any Number of Repetitions (anr), and the number of motifs was set as 10. The visualization of results was completed by TBtools (v2.080) (Chen et al. 2023).

Construction, quality control, and visualization of protein tertiary structure

The AlphaFold v2.3.2 monomer_casp14 model was employed to predict the structure of selected proteins from the TRE family at the tertiary level (Jumper et al. 2021). Default parameters were utilized, and the following database versions were accessed: uniport and uniref90 as of March

1, 2023, and pdb_mmcif and pdb_seqres as of March 3, 2023, with other databases using default versions. Swiss-Model online tool Structure Assessment was used for model visualization and quality control (Waterhouse et al. 2018), while QMEANDisCo was employed to assess the quality of the structural models (Studer et al. 2020). Tertiary structure models were compared using the structure comparison that is an online tool of Swiss-Model (https://swissmodel.expasy.org/comparison/).

RNA isolation, reverse transcription, and qRT-PCR

All samples were homogenized by a JXFSTPRP-24 tissue grinder (Jingxin, Shanghai, China), and RNA extraction was performed using a TRIzol reagent (Takara, Kyoto, Japan) according to the instructions. The purity and concentration of each RNA sample were measured with Nanodrop 2000 (Thermo Fisher Scientific, Waltham, MA, USA), and the integrity was assessed using a 1% agarose gel. Purified RNA was stored at − 80 °C for subsequent experiments.

Subsequently, the qualified RNA was used as a template to synthesize the first-strand complementary DNA (cDNA) with the PrimeScript RT reagent kit with gDNA Eraser (Takara, Kyoto, Japan) following the manufacturer's instructions and the cDNA was stored at − 20 °C. The cDNA template was diluted 3 times for qPCR.

HvRPL13 was used as the internal reference gene (Lu et al. 2019). All qPCR primers were designed using Primer Premier 5 software and used after specificity validation. Primer sequence details are shown in Table S1. The qRT-PCR was performed using TB Green Premix Ex Taq II (Tli RNaseH Plus) (Takara, Kyoto, Japan) according to the manufacturer's instructions in 20 µL volume. The qRT-PCR program was set as follows: Pre-denaturation was initiated at 95 °C for 5 min, proceeding to 39 cycles consisting of 95 °C for 5 s and 60 °C for 20 s. Subsequent to each cycle, the reaction mixture was elevated to 65 °C and maintained at this temperature for 5 s and then subjected to a continuous heating rate of 0.5 °C per second, while fluorescence was recorded to generate the melting curve. A single peak in the melt curve was deemed indicative of optimal amplification specificity. Finally, the $2^{-\Delta\Delta CT}$ was used to calculate the relative expression of genes.

Determination of carbohydrate content and trehalase activity

This part of the experiment was conducted according to the method described by Zhang (Zhang et al. 2017). In this study, 1 mL PBS was added to the samples after homogenization, followed by 30 min sonication, and 20 min centrifugation at 1,000 × g and 4 ℃. The supernatant was used to measure the contents of trehalose and glycogen. The remaining supernatant was ultracentrifuged for 60 min at 20,800 × g and 4 ℃ and then divided into supernatant and suspension (formed by adding 150 µL PBS to the precipitate) for measuring glucose content.

The amount of trehalose was detected using anthrone reagent. Briefly, 1% sulfuric acid (H_2SO_4, 30 µL) was added to the 30 µL sample, incubated for 10 min at 90 ℃ in a water bath, and 30% KOH (30 µL) was added after 3 min incubation in an ice bath. Developer (600 µL of 0.02 g anthrone in 100 mL 80% H_2SO_4) was added to a test tube containing the mixed solution, incubated in hot water (90 °C) for 10 min, then cooled on ice. The absorbance was measured at 630 nm. The glycogen and glucose were detected similarly; however, the sample of glycogen (160 µL) was first taken out and mixed with 32 µL of 0.1 U/L of amyloglucosidase (Sigma-Aldrich, Burlington, VT, USA) in a 1.5 mL Eppendorf (EP) tube. It was converted to glucose by incubating at 40 °C in a water bath for 4 h. In the next step, the glucose (Go) Assay Kit (Sigma-Aldrich, Burlington, VT, USA) was used to measure the levels of glucose, followed by the addition of 12 N H_2SO_4 (260 µL) to terminate the reaction. The absorbance was read at 540 nm.

RNA interference

The dsDNA fragments from the *HvTRE1-5* (*CL1187.contig1_All*) gene were amplified by PCR using specific primers containing the T7 promoter sequence at their 5' ends. The PCR amplification was carried out under the following conditions: preincubation at 95 °C for 3 min, 35 cycles at 95 °C for 30 s, 56 °C for 30 s, 72 °C for 1 min, and a last extension at 72 °C for 10 min. The purified amplification product of *HvTRE1-5* was used to synthesize dsRNA by in vitro transcription using the T7 RiboMax Express RNAi System (Promega, Madison, WI). The dsGFP, used as a control, was synthesized using a pMD-18 T plasmid containing the GFP sequence as the template, following the same methodology. The sense and anti-sense strands were first produced in two separate transcription procedures and then mixed for annealing. The reaction mixture was incubated at 70 °C for 10 min and then cooled in an ice bath for 20 min. The dsRNAs were then precipitated with 95% ethanol and 3 M sodium acetate (pH 5.2), washed with 70% ethanol, air-dried, and resuspended. The integrity and quantity of dsRNAs were evaluated with Nanodrop 2000 and by 1% agarose gel electrophoresis. The synthesized dsRNA was stored at − 80 °C.

The abdomen of each *H. vigintioctopunctata* larva (on the first day of the 4th instar) was injected with 2000 ng of dsHvTRE1-5 using a FemtoJet 4i (Eppendorf, Hamburg, Germany). The control groups were injected with dsGFP. Larvae collected at 24, 48, and 72 h post-injection were used to assess interference efficiency. Three biological replicates

were collected at each time point for both the experimental and control groups, with each replicate containing three larvae. Eighty larvae per treatment were injected for the observation of mortality.

Statistical analysis and visualization of data

Results were expressed as the mean ± standard error (SE) of independent replicates ($n \geq 3$). The data were analyzed using IBM SPSS statistics 26 software. Statistical significance was defined as $P < 0.05$. Tukey's test of one-way ANOVA was performed to test the significance of differences among treatments. GraphPad Prism version 9.0 software was employed to conduct the Mantel–Cox test for survival curve analysis. All figures and tables were produced using Microsoft Office 2022 and GraphPad 9.0 software.

Result

H. vigintioctopunctata fed on *P. floridana* showed a significantly reduced mortality rate and impaired development

We fed third-instar larvae of *H. vigintioctopunctata* with four different Solanaceae plants (Fig. 1a) named LK group

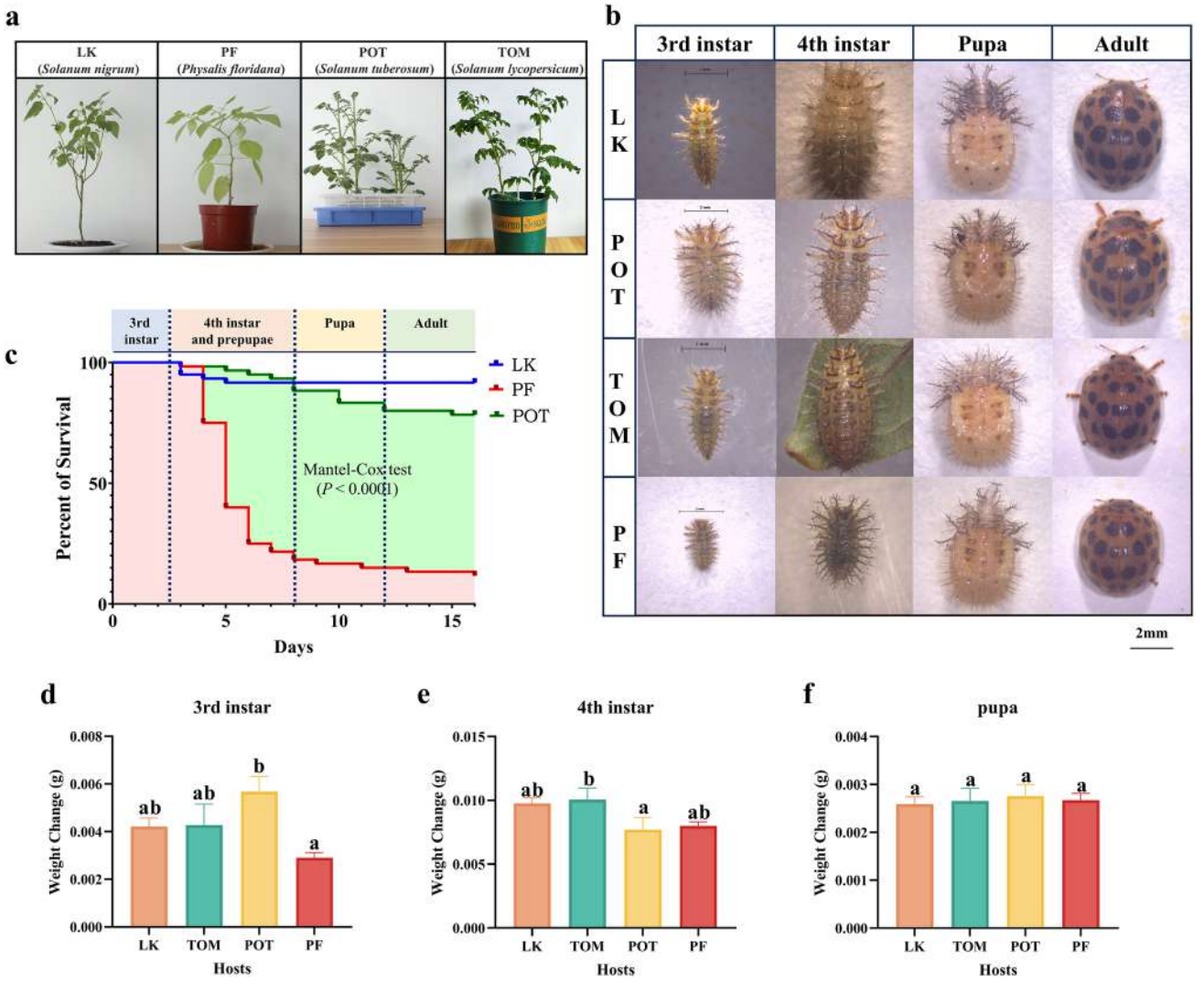

Fig. 1 Feeding on *P. floridana* causes abnormal development of *H. vigintioctopunctata* and causes extremely high mortality. **a** pictures of aerial parts of four host plants, *S. nigrum*, *P. floridana*, *S. tuberosum* and *S. lycopersicum*, from left to right; **b** the developmental stage bioassay of *H. vigintioctopunctata* fed on four host plants, from left to right, different developmental stages are indicated, and from top to bottom, different host plants are indicated. LK, POT, TOM and PF represent *S. nigrum*, *S. tuberosum*, *S. lycopersicum* and *P. floridana*, respectively; **c** survival of *H. vigintioctopunctata* as fed by *S. nigrum* (LK), *S. tuberosum* (POT) and *P. floridana* (PF); **d**, **e**, **f** represents the amount of body weight change in the different groups at the 3rd instar, 4th instar, and pupal stage, respectively

(*S. nigrum*), POT group (*S. tuberosum*), TOM group (*S. lycopersicum*), and PF group (*P. floridana*) and monitored their mortality rates. Observation results revealed that *H. vigintioctopunctata* larvae fed on *P. floridana* showed significantly smaller body size in the third and fourth instars compared to larvae fed on the other three host plants, but there was no apparent difference after pupation (Fig. 1b). Mortality rate analysis showed that *H. vigintioctopunctata* fed on *P. floridana* had a significantly higher mortality rate compared to the LK group, where the mortality rate was 8.3%, while for *P. floridana* it was 88.3% and interestingly, for the POT group, it was observed to be 18.97% at 16 days post-third molt (Fig. 1c). In the PF group, larvae began to exhibit substantial mortality at the end of the third instar, with the majority mortality during the fourth instar and prepupal stages. However, mortality events were notably less frequent during the pupal and adult stages. The results of weight change across various developmental stages reveal that the PF group exhibited the lowest weight change values at the third instar, significantly lower than those of the POT group (Fig. 1d). By the fourth instar, while no significant difference was observed between the PF and POT groups, the weight change in the PF group remained lower compared to both the LK and TOM groups, with a particularly notable distinction from the TOM group (Fig. 1e). Of importance, however, is the observation that during the pupal stage, the value of weight change was strikingly similar among all groups, showing negligible differences (Fig. 1f).

These findings signify that *P. floridana* markedly influences the survival and development of *H. vigintioctopunctata* larvae when acting as a host, while exhibiting no substantial effect on the survival of pupae or adults. Compared to the LK group, both POT and PF groups exhibited more pronounced changes in body size, accompanied by significant changes in weight. Conversely, the TOM group demonstrated performance nearly identical to that of the LK group.

Transcriptome reveals the effect of *P. floridana* as the host on the trehalose metabolism pathway of *H. vigintioctopunctata*

To explore the changes in *H. vigintioctopunctata* under different host feeding conditions, we performed transcriptome sequencing on *H. vigintioctopunctata* larvae across four treatment groups. Following transcriptome sequencing, with the LK group serving as the control, differential gene analysis was conducted. The number of differentially expressed genes in the PF, POT, and TOM groups sequentially decreased, totaling 3126, 1096, and 31 genes, respectively (Fig. S1). Using the LK group as a reference, we enriched 247, 219, and 39 differentially represented KEGG pathways in the PF, POT, and TOM groups, respectively. In particular, within the "Starch and Sucrose Metabolism" pathway (Pathway: ko00500), we identified and enriched 66 genes that were significant differential expression. Among the 66 genes enriched in the "starch and sucrose metabolism" pathway, using the LK group as the control, the PF group exhibited the highest number of differentially expressed genes (DEGs), totaling 30, whereas the TOM group showed the least, with only 7 (Fig. S2). These results suggest relatively minor differences between *H. vigintioctopunctata* in LK and TOM groups but significant differences in the pattern of enrichment genes among the PF and POT groups (Fig. 2a), indicating varying impacts of different plant diets on carbohydrate metabolism in *H. vigintioctopunctata*. Trehalose, functioning as an insect blood sugar, plays a crucial role in insect energy metabolism, with trehalases serving as vital enzymes in trehalose metabolism (Fig. 2b)(Shukla et al. 2015). Of the 66 genes showing enrichment in the "starch and sucrose metabolism pathway," annotation uncovered eight distinct trehalase (TRE) transcripts, emphasized in red within Fig. 4a. Notably, when fed on *P. floridana*, marked differences in expression emerged: *HvTRE1-3* (*Unigene5944_All*) displayed significant upregulation ($P < 0.01$), whereas *HvTRE1-5* (*CL1187.contig1_All*) was significantly downregulated ($P < 0.01$), in comparison to a *S. nigrum* diet (Fig. 2c). Considering the incomplete structure of *HvTRE1-3* (*Unigene5944_All*) which may not confer full trehalase functionality (Fig. 4b), in this study, we have elected to focus on *HvTRE1-5* (*CL1187.contig1_All*) as our subject of investigation.

Consistent with the results from bioassays, the PF and POT groups showed considerable transcriptomic differences compared to the LK group, whereas only 31 differentially expressed genes were identified between the TOM and LK groups, indicating a high degree of similarity between these two treatments. Consequently, in subsequent experiments, we will proceed with the LK group as the control, focusing on the POT and PF groups to investigate the effects of these three host plants on *H. vigintioctopunctata*. This approach aims to delve further into the impacts of dietary variation on the insect's physiology and metabolism.

Analysis of *HvTRE* family and TRE evolution in ladybird beetles (*Coleoptera*: *Coccinellidae*)

Given that the trehalase genes of *H. vigintioctopunctata* had not been previously identified or published, to ensure the accuracy and feasibility of our experiment, we proceeded to further validate the eight trehalase transcripts obtained through annotation. To identify TRE transcripts and verify their relationships, we conducted a multi-level structural analysis of annotated transcripts and compared them with TRE family members of other ladybird beetle species. We compared the protein sequences of TRE family members

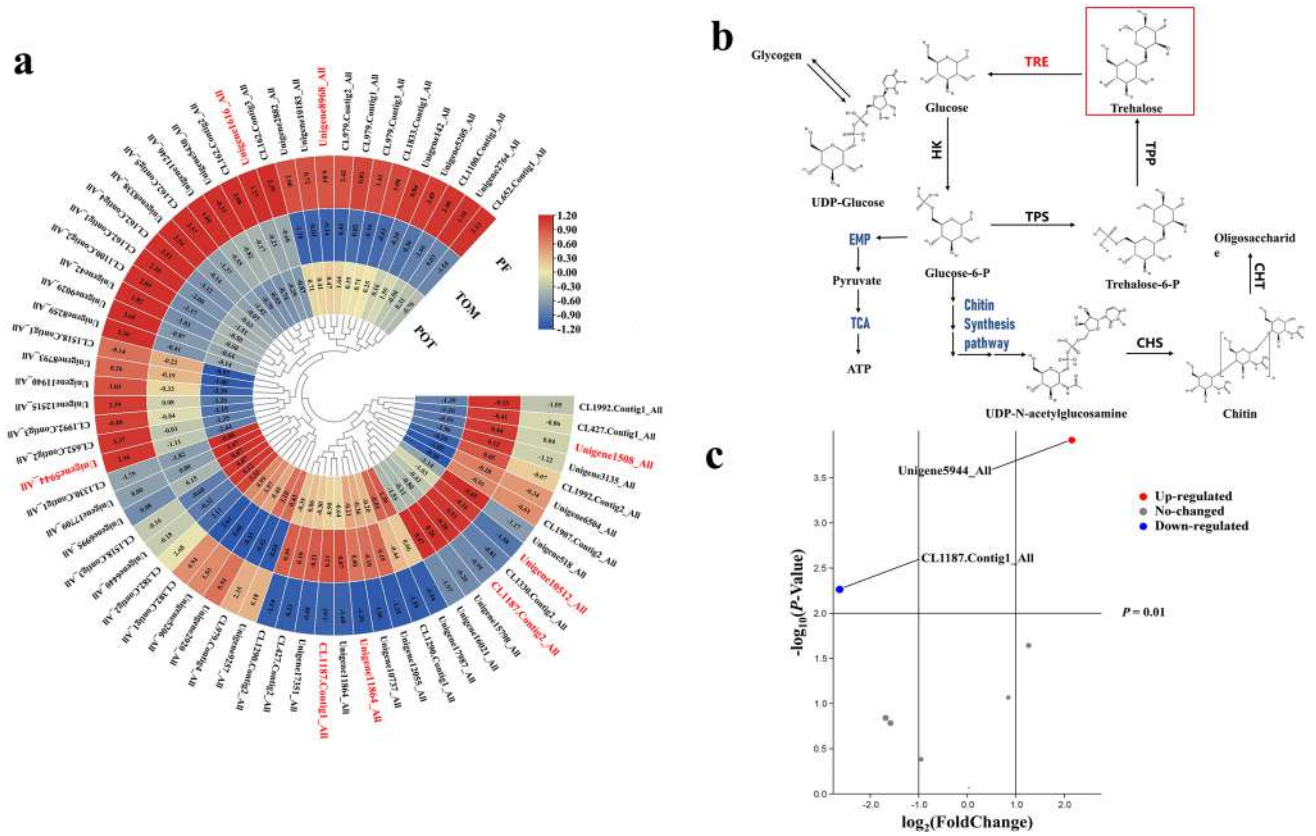

Fig. 2 Different host plants cause changes in glucose metabolism pathways at the transcriptional level of *H. vigintioctopunctata*. **a** heat maps of the expression of 66 genes enriched in the "starch and sucrose metabolism" pathway were plotted using the mean of $\log_2$foldchange, which was calculated using the LK group as the reference; **b** schematic representation of the trehalose metabolic pathway, **c** volcano plot of eight *H. vigintioctopunctata* trehalase transcripts

from *H. axyridis*, *C. septempunctata*, *P. japonica*, *C. montrouzieri*, and *H. vigintioctopunctata* and completed the phylogenetic construction. Notably, we included the TRE family protein sequences of the model beetle *T. castaneum* and the important pest insect *N. lugens* as outgroups in tree construction, aiding in the identification of TRE family characteristics in ladybird beetles.

The entire phylogenetic tree is divided into 3 main branches (Fig. 3a), which we categorize as purple, yellow, and green arcs. Each major branch contains corresponding trehalases in 5 ladybird beetle species, demonstrating the relatively weak species specificity of trehalases. Notably, one branch is exclusive to the ladybird beetle family (green arc), while the trehalase family members for *T. castaneum* and *N. lugens* are not present, suggesting that ladybird beetles may have evolved a unique trehalase branch to adapt to their specific morphology and developmental processes. Furthermore, trehalases are classified into two major types: membrane-bound trehalases and soluble trehalases. After predicting the transmembrane structures of a total of 51 TRE protein family members, we identified members potentially bound to membranes and their binding modes and sites (Table S2), marking the corresponding members with red pentagrams on the evolutionary tree. Interestingly, one sub-branch of the yellow arc in the evolutionary tree consists of one membrane-bound trehalase member from each of the 7 species, while some predicted members with membrane-binding domains are scattered across the other two main branches. This further illustrates the interspecies conservation of trehalases while indicating that the differences between different subtypes of trehalases are greater than interspecies differences.

The motif enrichment analysis results of the trehalase family members (Fig. 3b) show consistent findings. All trehalases share similar motif compositions, with some members like *Nlug017628* and *Unigene8968_All* missing motif4 at the N-terminus. Both *AFT92044.1* and *CL1187.Contig1_All* are lacking Motif 2 at their C-terminal ends. Through examination of the tertiary structure models, it is observed that the structures formed by the N-terminus and C-terminus of the TREs appear irregular. Despite this variability in structure, their functional performance remains unaffected.

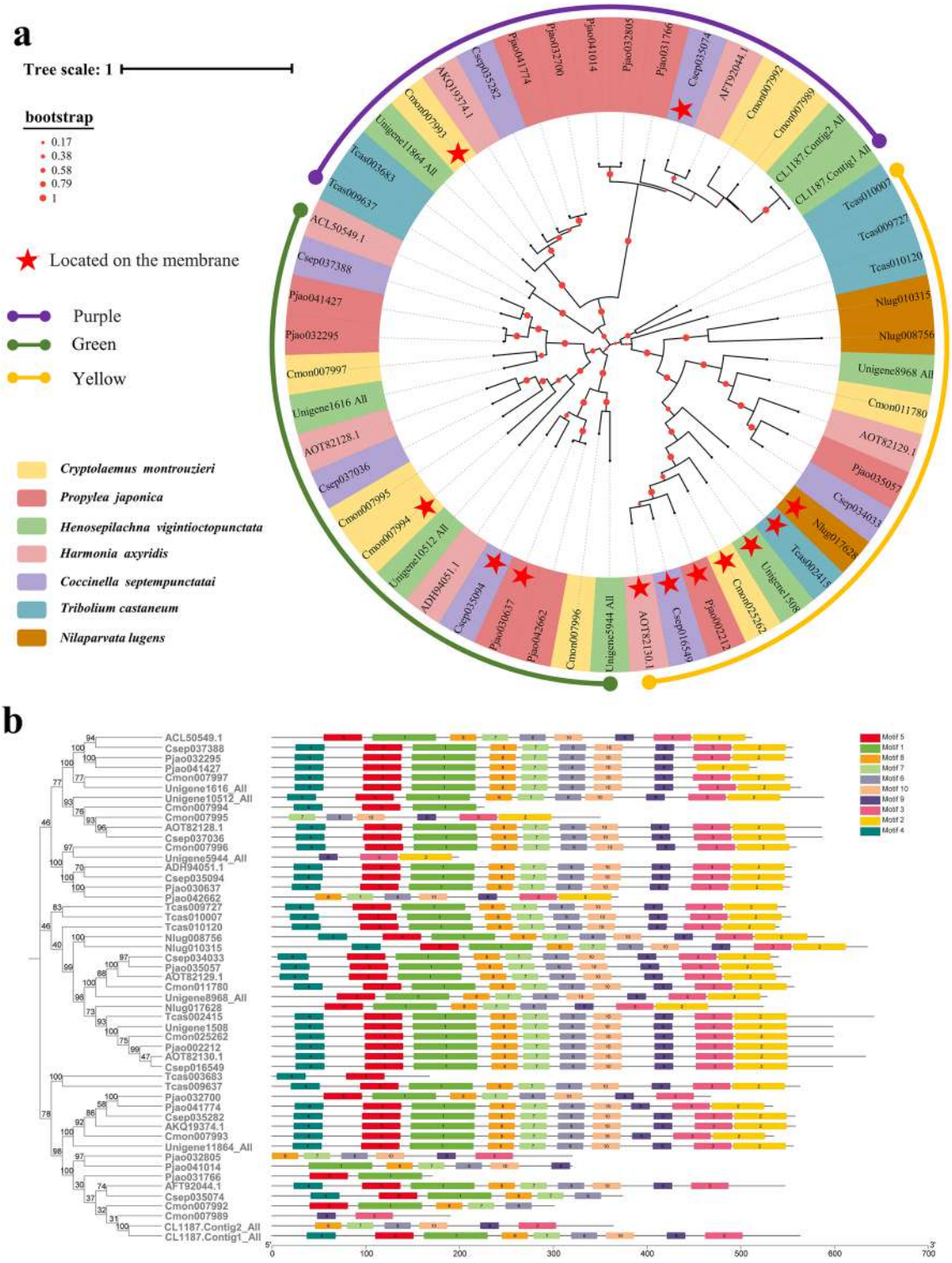

Fig. 3 Evolutionary analysis of TRE proteins from seven insect species. **a** protein evolutionary tree of TRE family in seven insect species. Three arcs in purple, green, and yellow denote the ranges of the three main clades of the phylogenetic tree, while red star symbols indicate those TRE members that are localized to the membrane in subcellular localization analysis; **b** motif sequence structure diagram of TRE protein family members, protein sequence evolutionary tree on the left, motif sequence structure of corresponding sequences on the right, different colors represent different motifs, and sequence length scale on the bottom. All the details of the motifs are shown in Fig. S3

This observation underscores the conservation of trehalases in different species, particularly within the *Coccinella*.

Based on the evolutionary relationships and adopting the nomenclature method of *H. axyridis* TREs, we named the eight *HvTRE* transcripts as illustrated in Table 1.

At the tertiary level, we used AlphaFold 2.0 to perform structural simulations on members of the TRE family in the ladybird beetles family, which have relatively complete secondary structures. We conducted quality assessments on all models to ensure the reliability of the structural models (Fig. S4). Our structural modeling results indicate that the majority of trehalose enzymes exhibit conservative tertiary structures (Fig. 4a), with the overlapping regions primarily concentrated in the central region of the protein sequences, showing significant differences in the N-terminal regions among different members. However, the overlapping regions of TRE protein members from four different ladybird beetles are almost identical (Fig. 4b), suggesting that these regions may serve as conservative functional regions or important ligand binding sites in the trehalose hydrolysis process.

The host *P. floridana* influences the expression of *HvTRE1-5* and *H. vigintioctopunctata* trehalose metabolism.

Based on the results from the differential expression gene screening in the transcriptome and the identification and structural analysis of *H. vigintioctopunctata* trehalase enzymes, *HvTRE1-5* (*CL1187.Contig 1_All*) was chosen as the subject of study to investigate its variations and functions under different host feeding conditions. Trehalose, an essential blood sugar for insects, plays a crucial role

Table 1 Table of *HvTRE* Transcripts names and annotations

Gene ID	Name	SwissProt description	Pfam description
Unigene10512_All	*HvTRE1-1*	Trehalase OS = Tenebrio molitor OX = 7067 PE = 2 SV = 1	Trehalase
Unigene1616_All	*HvTRE1-2*	Trehalase OS = Tenebrio molitor OX = 7067 PE = 2 SV = 1	Trehalase
Unigene5944_All	*HvTRE1-3*	Trehalase OS = Pimpla hypochondriaca OX = 135,724 GN = tre1 PE = 1 SV = 1	Trehalase
Unigene11864_All	*HvTRE1-4*	Trehalase OS = Tenebrio molitor OX = 7067 PE = 2 SV = 1	Trehalase
CL1187.Contig1_All	*HvTRE1-5*	Trehalase OS = Apis mellifera OX = 7460 PE = 1 SV = 1	Trehalase
CL1187.Contig2_All	*HvTRE1-5 X1*	Trehalase OS = Apis mellifera OX = 7460 PE = 1 SV = 1	Trehalase
Unigene8968_All	*HvTRE2-1*	Trehalase OS = Tenebrio molitor OX = 7067 PE = 2 SV = 1	Trehalase
Unigene1508_All	*HvTRE2-2*	Trehalase OS = Tenebrio molitor OX = 7067 PE = 2 SV = 1	Trehalase

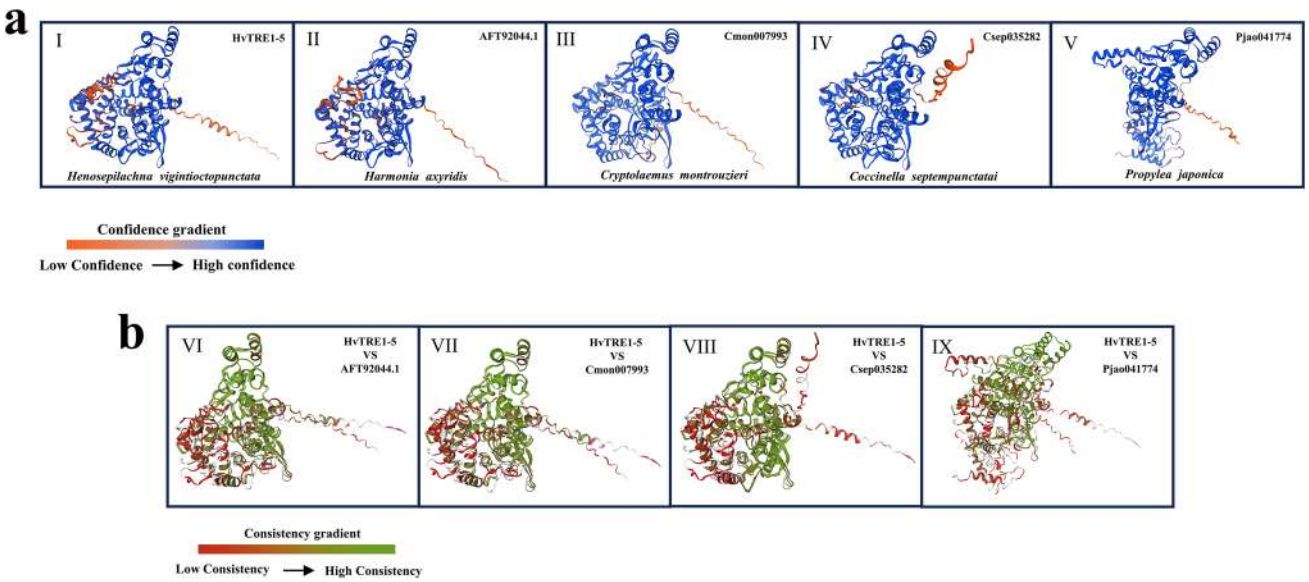

Fig. 4 Structure of TRE proteins from five ladybird species. **a** TRE predicted protein structures derived from five ladybird species, with bluer color indicating higher confidence and redder color indicating lower confidence; **b** comparison of TRE protein structure between four different species and *CL1187.Contig1*. The greener the color, the higher the consistency, and the red the lower the consistency

in their growth, development, and stress resistance. The trehalase is key in regulating trehalose levels in insects. To investigate the impact of different host plants on the trehalose metabolism of *H. vigintioctopunctata*, we fed 3rd instar larvae with leaves from different host plants and sampled them from the 4th instar molting until pupation for 24 h. We measured the relative expression levels of *HvTRE1-5*, trehalose, glucose, glycogen content, and the activities of soluble and membrane-bound trehalase at each time point (Fig. 5).

At different developmental stages, significant differences are observed in the relative expression levels of *HvTRE1-5* in *H. vigintioctopunctata*. Particularly during the fourth instar stage, *HvTRE1-5* shows extremely low relative expression levels, which significantly increase after 24 h in the prepupal stage and further rise post-pupation. Although this increasing expression pattern with developmental progression is nearly identical across three different host feeds, the feeding of different hosts significantly impacts the relative expression levels of *HvTRE1-5*. Notably, during the prepupal and post-pupal stages, PF and POT groups larvae exhibit

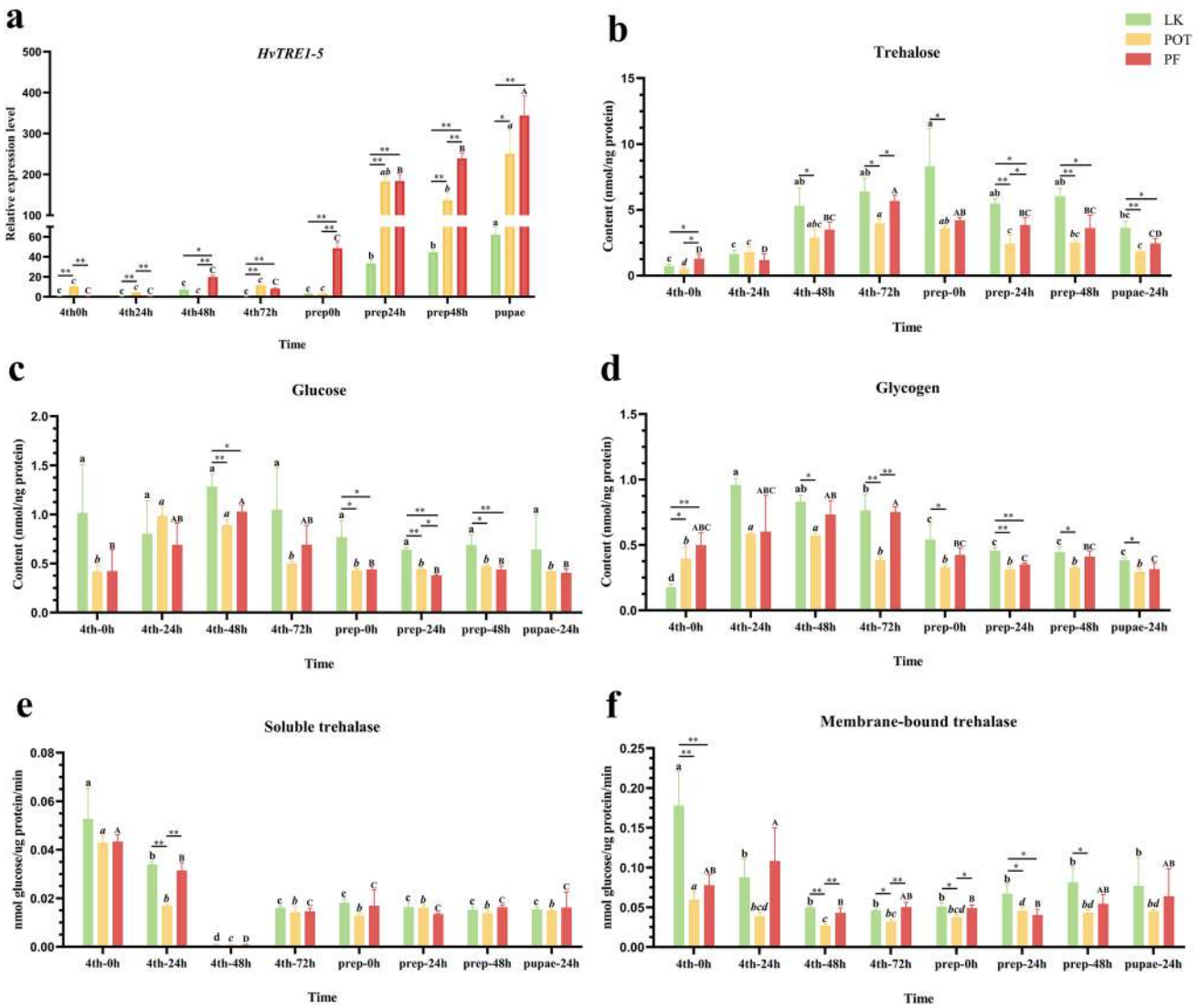

Fig. 5 Changes in trehalose metabolism of *H. vigintioctopunctata* at different developmental times fed by different hosts. **a** temporal expression profile of *HvTRE1-5* under different host feedings; **b**, **c** and **d** represent the trehalose, glucose and glycogen contents of *H. vigintioctopunctata* at different times fed by different hosts, and **e** and **f** represent the soluble trehalase and membrane-bound trehalase activities of *H. vigintioctopunctata* at different times fed by different hosts. Groups fed by different host plants are indicated using different colored columns. Different letters on the columns indicate significant differences in different periods under the same host ($P < 0.05$), while * indicates significant differences in that period between the two hosts at either end of the horizontal line (* means $P < 0.05$, ** means $P < 0.01$)

much higher relative expression levels compared to the LK group (Fig. 5a).

On the trehalose content, the trends of *H. vigintioctopunctata* larvae fed on three different host plants are similar, with trehalose content increasing with developmental time and reaching its peak at the time of cessation of feeding (4th-72 h and prep-0 h), followed by a gradual decrease. Throughout the entire time range, larvae in the LK group consistently exhibit higher trehalose levels at almost all time points compared to those fed on *S. tuberosum* and *P. floridana*, while the trehalose content in the PF group is slightly higher than that in the POT group, with this difference being most pronounced during the prepupal and pupal stages (Fig. 5b). Regarding glucose content, *H. vigintioctopunctata* larvae fed on the three different host plants show an increase in glucose levels during the pre-4th instar period, reaching a peak at the 4th instar 48 h, followed by a decline, and maintaining stability during the prepupal stage. Similar to the trehalose content results, throughout the entire time range, larvae in the LK group exhibit higher glucose levels compared to those in the POT and PF groups, while there is almost no significant difference in glucose content between the POT and PF groups (Fig. 5c). The trend in glycogen content follows a similar pattern to glucose content, showing an upward trend during the early 4th instar period, reaching its peak in the 4th instar at 24–48 h, and subsequently gradually decreasing, maintaining equilibrium during the prepupal stage. In contrast to trehalose and glucose, glycogen content in the LK and PF groups is more similar, being significantly higher than that in the POT group during the late 4th instar and prepupal stages (Fig. 5d).

Soluble trehalase and membrane-bound trehalase are two subtypes of trehalase enzymes. Soluble trehalase activity gradually decreases from the 4th instar larvae and nearly disappears by the 4th instar 48 h. However, the activity of soluble trehalase recovers and remains stable on the 4th instar within 72 h. When fed on three different host plants, significant differences were observed between the PF group and LK group compared to the POT group only at 24 h into the 4th instar stage, with no notable variances observed at other times (Fig. 5e). In contrast to soluble trehalase, the activity of membrane-bound trehalase decreases initially during the 4th instar stage and then stabilizes, with no significant changes observed on the 4th instar 48 h. Under the feeding conditions of three different host plants, the membrane-bound trehalase activity of POT group larvae is significantly lower during the late 4th instar stage and prepupal stage compared to other groups of larvae (Fig. 5f).

These results suggest that feeding on different host plants affects the trehalose metabolism and sugar accumulation in *H. vigintioctopunctata*. Specifically, feeding on *P. floridana* significantly influences the trehalose metabolism of *H. vigintioctopunctata* during the prepupal stage.

HvTRE1-5 plays an important role in the pupation of *H. vigintioctopunctata*

The previous findings indicate that a diet of *P. floridana* affects the growth and development of *H. vigintioctopunctata*, as well as the trehalose metabolism and carbohydrate accumulation during the pupation process of *H. vigintioctopunctata*. To further investigate the function of *HvTRE1-5* in *H. vigintioctopunctata*, dsHvTRE1-5 was synthetically designed for RNA interference in *H. vigintioctopunctata* larvae, with dsGFP serving as the control. Based on the temporal expression profile (Fig. 5a), the injection time was chosen as 24 h after the 4th instar. 48 h post-dsHvTRE1-5 injection, the expression level of *HvTRE1-5* in the dsHvTRE1-5 treatment group was significantly lower compared to the dsGFP control group (Fig. 6b), with an interference efficiency of 58.8%, indicating the effectiveness of dsHvTRE1-5. In the dsHvTRE1-5 treatment group, the mortality rate of *H. vigintioctopunctata* reached 52.5% within 10 days, significantly higher than the control group with dsGFP, which was 22.5% (Fig. 6c). It is noteworthy that the time of death of all individuals in the dsHvTRE1-5 treatment group was concentrated in the prepupal stage, whereas for GFP, the death time was concentrated during the pupae stage. This demonstrates the significant importance of *HvTRE1-5* for the pupation of *H. vigintioctopunctata* and its high expression during the prepupal stage.

Following the knockdown of *HvTRE1-5*, significant upregulation was observed for *HvTRE1-1*, *HvTRE1-4*, and *HvTRE2-1* (Fig. 6e, h, and j), whereas *HvTRE1-5 X1* and *HvTRE2-2* showed a marked decrease in their relative expression levels (Fig. 6i and k). In contrast, *HvTRE1-2* and *HvTRE1-3* exhibited no evident changes (Fig. 6f and g). The upregulation of multiple *HvTREs* to some extent compensates for the reduction in trehalase activity caused by the downregulation of *HvTRE1-5*.

Discussion

The interaction between plants and herbivorous insects is one of the most classic examples of coevolution in nature, and the use of plants as a source of insect-resistant substances has a long history (Xu et al. 2019; Wu et al. 2021). Understanding the effects of plants with insect resistance on pests helps us understand the relationship between plants and herbivores and also provides a new source and theoretical basis for the development of plant-derived pesticides. In this study, we discussed the potential of the genus *Physalis* plant *P. floridana* as a source for developing plant-based pesticides and explored its effects on the mortality of *H.*

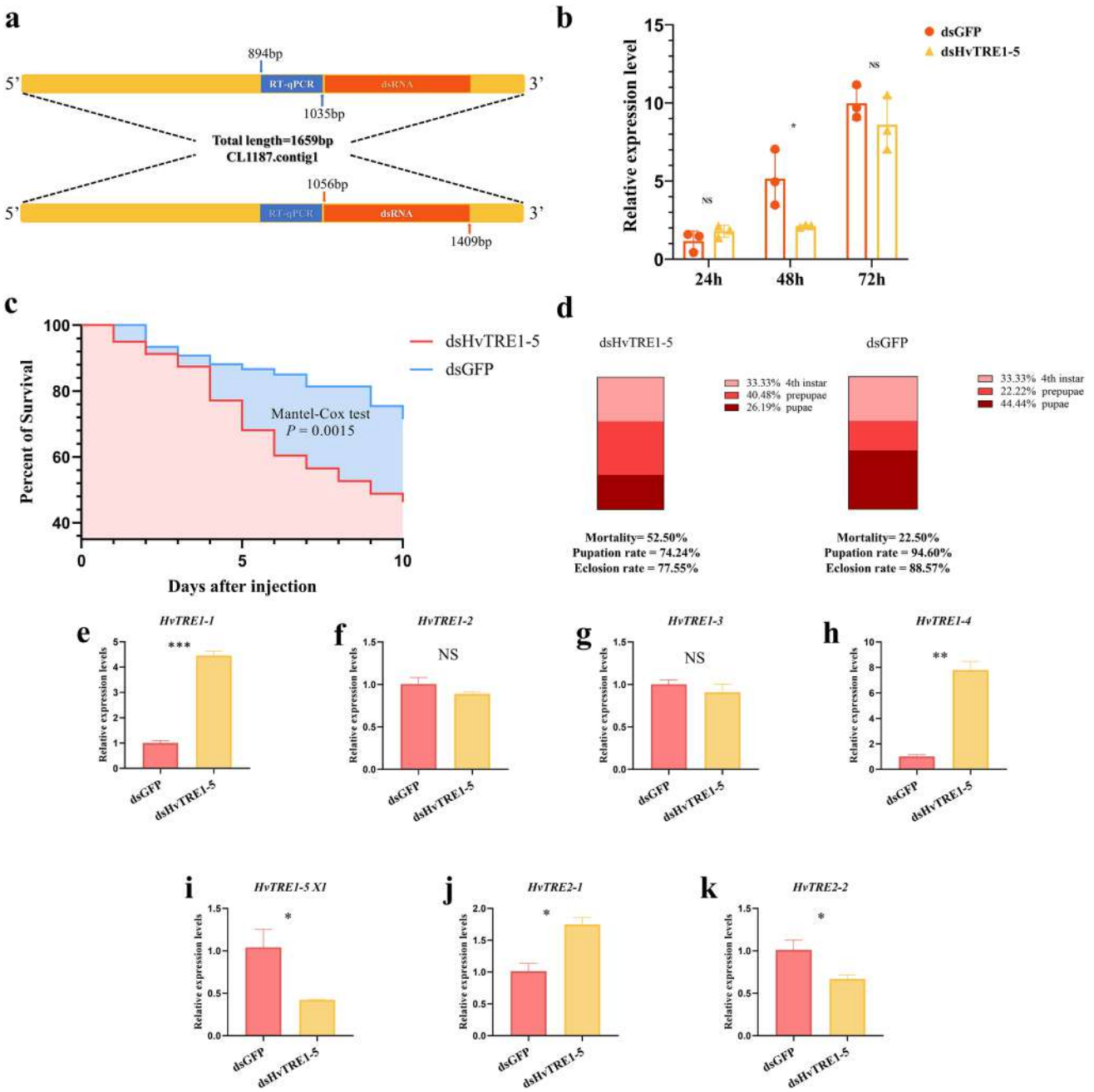

Fig. 6 Knockdown of HvTRE1-5 caused a significant increase in *H. vigintioctopunctata* mortality. **a**: Schematics of double-stranded RNA and RT-qPCR primer design patterns, **b** relative expression levels of *HvTRE1-5* between dsHvTRE1-5 and control within 72 h of injection, **c** survival of *H. vigintioctopunctata* as treated by dsHvTRE1-5 and dsGFP, **d** distribution of developmental stages at *H. vigintioctopunctata* death under dsHvTRE1-5 versus dsGFP treatment. **e**, **f**, **g**, **h**, **i**, **j**, **k**, respectively, denote the relative expression levels of genes *HvTRE1-1*, *HvTRE1-2*, *HvTRE1-3*, *HvTRE1-4*, *HvTRE1-5 X1*, *HvTRE2-1*, and *HvTRE2-2*, following 48-h treatments with dsTRE1-5 and dsGFP

vigintioctopunctata as well as its impact on carbohydrate metabolism.

Plants in *Physalis* genus are a typifier of Solanaceae, containing a rich variety of chemical compounds such as steroidal compounds (primarily physalins and withanolides), flavonoids, terpenoids, alkaloids, organic acids, and other compounds, endowing them with the potential for development as biopesticides (Popova et al. 2020a, b). Researchers, led by Elliger, observed strong developmental inhibitory effects on *Helicoverpa zea* larvae when treated with leaf extracts of *Physalis peruviana* (Elliger and Waiss 1989). The treatment of *Rhodnius prolixus* with Physalins,

a unique secondary metabolite of *Physalis*, extracted from *Physalis angulata*, resulted in significant growth inhibition, and multiple members of Physalins could induce immunosuppression (Castro et al. 2008, 2009). Then the infection with *Trypanosoma rangeli* results in *R. prolixus* death (Garcia et al. 2006). Additionally, apart from the significant growth inhibitory effects, high concentrations of 4β-hydroxywithanolide and withanolide E, present in the leaves and fruits of *P. peruviana*, have been demonstrated to possess inhibition of feeding function (Yang et al. 2020).

In this study, we examined the effects of the important horticultural pest *H. vigintioctopunctata* feeding on different Solanaceae host plants, specifically *P. floridana*. Our results show that feeding on *P. floridana* significantly impacts larval growth and size, leading to high larval mortality. In contrast, feeding on tomato and potato leaves does not have the same detrimental effects. These findings suggest that *P. floridana*, like other members of the *Physalis* genus, exhibits strong insect resistance and potential as a plant-based insecticide source.

Trehalose is crucial for insects, constituting 80–90% of the total blood carbohydrate in their hemolymph. Despite the well-known synthesis pathways, further research is needed to fully understand its impact on insects. The metabolic role of trehalose extends beyond energy metabolism, attracting attention to its influence on endogenous hormones and development. For instance, *Apolygus lucorum* has been found that ecdysone and ecdysone receptors regulate the transcription of *TRE1*, affecting trehalose metabolism (Tan et al. 2015). Another significant aspect of trehalose for insects is its protective function, aiding insect adaptation to stress (Thorat et al. 2016; Tellis et al. 2023a, b). Previous studies have demonstrated its pivotal role in insect responses to abiotic stresses such as cold, heat, heavy metals, and low oxygen, as well as biotic stresses like fungal infections (Chen et al. 2003; Wang et al. 2017; Perez and Aron 2023; Wan et al. 2023a, b; Zhang et al. 2023). In this study, 8 trehalase transcript variants were identified for the first time in *H. vigintioctopunctata*, and a temporal expression profile was constructed for *HvTRE1-5* showing significantly different expression when larvae fed on *P. floridana* and *S. tuberosum* compared to *S. nigrum* leaf feeders. Subsequent measurement of carbohydrate content and trehalase activities in *H. vigintioctopunctata* larvae fed on different host plants revealed higher total carbohydrate content and catalytic trehalase activity in those fed on *S. nigrum*. These findings indicate significant influences of different host plants on trehalose metabolism in *H. vigintioctopunctata* larvae. The effects might stem from variations in plant nutrients on one hand and the potential presence of antifeedant secondary metabolites in *P. floridana* on the other, leading to altered larval feeding patterns. Moreover, RNAi-mediated knockdown of *HvTRE1-5* resulted in a significant increase in mortality rates during the prepupal stage, further validating the significance of *HvTRE1-5* in the pupation process.

It is important to note that the nutritional conditions experienced by *H. vigintioctopunctata* under different host plants vary, which in turn can influence their carbohydrate content. Thus, changes in total carbohydrate levels cannot be solely attributed to variations in the relative expression of *HvTRE1-5*. Furthermore, many insects possess multiple *TRE* genes, and studies have demonstrated that different *TRE* transcripts can be expressed differently over time and across tissues (Zhou et al. 2019; Yu et al. 2021; Zhang et al. 2022). Frequently, it is not a single trehalase that mediates all functions. In our study, the discrepancies observed in trehalase activity were less pronounced compared to the changes in the relative expression of *HvTRE1-5*, suggesting that *HvTRE1-5* may not be the predominant gene driving trehalase activity. The RNAi results, however, highlight a vital role for *HvTRE1-5* in the pupation process of *H. vigintioctopunctata*, indicating its importance despite potentially not being the most active member of the trehalase family.

Overall, the significant lethal effects of *P. floridana* on *H. vigintioctopunctata* demonstrate its strong potential for development as a botanical insecticide. The impact on the prepupal stage of *H. vigintioctopunctata* is likely attributed to the regulation of the trehalase *HvTRE1-5* by *P. floridana*. However, the high mortality rate of *H. vigintioctopunctata* due to *P. floridana* may have other essential origins, since after successful pupation, *P. floridana* loses its significant lethality. Castro et al. mentioned that Physalins compounds could have a potent impact on the insect immune system and lead to pest mortality (Castro et al. 2008, 2009), and since *P. floridana* also contains abundant Physalins compounds, further research is warranted on their immunological effects on *H. vigintioctopunctata*. Additionally, it remains to be investigated whether the extracts can exhibit significant control effects on other pests, which serves as a crucial basis for developing it as a botanical insecticide. In conclusion, our research shows that *P. floridana* holds potential for further development as a green insecticide for combating *H. vigintioctopunctata* and other pests.

Supplementary Information The online version contains supplementary material available at https://doi.org/10.1007/s10340-024-01826-6.

Author contributions Resources were provided by H.W. and S.W.; J.L., B.T., and X.W. designed the experiments; X.W., B.H., S.W., T.W., and L.Y. performed the experiments; X.W. and J.L. performed the data analysis; X.W. wrote the original manuscript; and J.L. and B.T. reviewed and revised the manuscript. All authors commented on previous versions of the manuscript, and all authors have read and agreed to the published version of the manuscript.

Funding This work was supported by the National Natural Science Foundation of China (31970346 and 31470407).

Data availability No datasets were generated or analyzed during the current study.

Declarations

Conflict of interests The authors declare no competing interests.

Ethics approval This is an observational study. The Hangzhou Normal University Research Ethics Committee has confirmed that no ethical approval is required.

References

Anders S, Huber W (2010) Differential expression analysis for sequence count data. Genome Biol 11(10):R106. https://doi.org/10.1186/gb-2010-11-10-r106

Bailey TL, Boden M, Buske FA, Frith M, Grant CE, Clementi L, Ren J, Li WW et al (2009) MEME SUITE: tools for motif discovery and searching. Nucleic Acids Res 37:W202–W208. https://doi.org/10.1093/nar/gkp335

Burgueno AP, Amoros ME, Deagosto E, Davyt B, Diaz M, Gonzalez A, Rossini C (2023) Preference and performance in an herbivorous coccinellid beetle: a comparative study of host plant defensive traits, insect preference, and survival. Arthropod-Plant Interact. https://doi.org/10.1007/s11829-023-10004-x

Castro DP, Figueiredo MB, Genta FA, Ribeiro IM, Tomassini TC, Azambuja P, Garcia ES (2009) Physalin B inhibits *Rhodnius prolixus* hemocyte phagocytosis and microaggregation by the activation of endogenous PAF-acetyl hydrolase activities. J Insect Physiol 55(6):532–537. https://doi.org/10.1016/j.jinsphys.2009.01.013

Castro DP, Figueiredo MB, Ribeiro IM, Tomassini TC, Azambuja P, Garcia ES (2008) Immune depression in *Rhodnius prolixus* by seco-steroids, physalins. J Insect Physiol 54(3):555–562. https://doi.org/10.1016/j.jinsphys.2007.12.004

Chen C, Wu Y, Li J, Wang X, Zeng Z, Xu J, Liu Y, Feng J et al (2023) TBtools-II: A one for all, all for one bioinformatics platform for biological big-data mining. Mol Plant 16(11):1733–1742. https://doi.org/10.1016/j.molp.2023.09.010

Chen Q, Behar KL, Xu T, Fan C, Haddad GG (2003) Expression of *Drosophila* trehalose-phosphate synthase in HEK-293 cells increases hypoxia tolerance. J Biol Chem 278(49):49113–49118. https://doi.org/10.1074/jbc.M308652200

Chen Y, Chen Y, Shi C, Huang Z, Zhang Y, Li S, Li Y, Ye J et al (2018) SOAPnuke: a MapReduce acceleration-supported software for integrated quality control and preprocessing of high-throughput sequencing data. GigaScience 7(1):1–6. https://doi.org/10.1093/gigascience/gix120

Dyer LA, Dodson CD, Gentry G (2003) A bioassay for insect deterrent compounds found in plant and animal tissues. Phytochem Anal 14(6):381–388. https://doi.org/10.1002/pca.734

Elliger CA, Waiss A (1989) Insect growth inhibitors from Petunia and other solanaceous plants. ACS Symp Ser American Chem Soc 387:188–205. https://doi.org/10.1021/bk-1989-0387.ch014

Galand G (1989) Brush border membrane sucrase-isomaltase, maltase-glucoamylase and trehalase in mammals. Comparative development, effects of glucocorticoids, molecular mechanisms, and phylogenetic implications. Comparative biochemistry and physiology. B Comparative Biochem 94(1):1–11. https://doi.org/10.1016/0305-0491(89)90002-3

Garcia ES, Castro DP, Ribeiro IM, Tomassini TC, Azambuja P (2006) Trypanosoma rangeli: effects of physalin B on the immune reactions of the infected larvae of *Rhodnius prolixus*. Exp Parasitol 112(1):37–43. https://doi.org/10.1016/j.exppara.2005.09.003

Gong P, Song C, Liu H, Li P, Zhang M, Zhang J, Zhang S, He C (2021) *Physalis floridana* CRABS CLAW mediates neofunctionalization of *GLOBOSA* genes in carpel development. J Exp Bot 72(20):6882–6903. https://doi.org/10.1093/jxb/erab309

Guo M, Nanda S, Yang C, Li Z, Liu J, Gao R, Zhang Y, Zhou X et al (2023) Oral RNAi assays in *Henosepilachna vigintioctopunctata* suggest *HvSec23* and *HvSar1* as promising molecular targets for pest control. Entomol Gen 43(1):147–155. https://doi.org/10.1127/entomologia/2023/1712

Januario AH, Filho ER, Pietro RCLR, Kashima S, Sato DN, Franca SC (2002) Antimycobacterial physalins from *Physalis angulata* L. (Solanaceae). Phytotherapy Res: PTR 16(5):445–448. https://doi.org/10.1002/ptr.939

Jumper J, Evans R, Pritzel A, Green T, Figurnov M, Ronneberger O, Tunyasuvunakool K, Bates R et al (2021) Highly accurate protein structure prediction with AlphaFold. Nature 596(7873):583–589. https://doi.org/10.1038/s41586-021-03819-2

Letunic I, Bork P (2007) Interactive Tree Of Life (iTOL): an online tool for phylogenetic tree display and annotation. Bioinformatics 23(1):127–128. https://doi.org/10.1093/bioinformatics/btl529

Liu J, Jiang D (2014) Research advance on trehalose synthesis related genes in crops. Genomics Appl Biol 33(2):432–437. https://doi.org/10.5555/20143178927

Lu J, Chen S, Guo M, Ye C, Qiu B, Wu J, Yang C, Pan H (2019) Selection and validation of reference genes for RT-qPCR analysis of the ladybird beetle *Henosepilachna vigintioctopunctata*. Front Physiol. https://doi.org/10.3389/fphys.2019.00981

Lu J, Luo M, Wang L, Li K, Yu Y, Yang W, Gong P, Gao H et al (2021) The *Physalis floridana* genome provides insights into the biochemical and morphological evolution of *Physalis* fruits. Hortic Res. https://doi.org/10.1038/s41438-021-00705-w

Luo Y-J, Chen Y, Wang X-J, Wang S-T, Yang Y-Y, Xu H-X, Qu C, Wu Y et al (2022) Validamycin affects the development and chitin metabolism in *Spodoptera frugiperda* by inhibiting trehalase activity. Entomol Gen 42(6):931–939. https://doi.org/10.1127/entomologia/2022/1608

Masoumi Z, Noghabi SS, Izadi H (2021) Trehalose and proline failed to enhance cold tolerance of the cowpea weevil Callosobruchus maculatus (F.) (Col.: Bruchidae). J Stored Prod Res. https://doi.org/10.1016/j.jspr.2021.101853

Mei Y, Jing D, Tang S, Chen X, Chen H, Duanmu H, Cong Y, Chen M et al (2022) InsectBase 2.0: a comprehensive gene resource for insects. Nucleic Acids Res 50(D1):D1040–D1045. https://doi.org/10.1093/nar/gkab1090

Murungi LK, Kirwa H, Salifu D, Torto B (2016) Opposing roles of foliar and glandular trichome volatile components in cultivated nightshade interaction with a specialist herbivore. PLoS ONE. https://doi.org/10.1371/journal.pone.0160383

Perez R, Aron S (2023) Protective role of trehalose in the Namib desert ant *Ocymyrmex robustior*. J Exp Biol. https://doi.org/10.1242/jeb.245149

Popova V, Stoyanova A, Mazova N (2020a) Phytochemical composition and biological activity of *Physalis* spp.: a mini- review. Food Sci Appl Biotechnol. https://doi.org/10.30721/fsab2020.v3.i1.80

Popova V, Stoyanova A, Mazova N (2020b) Phytochemical composition and biological activity of *Physalis* spp.: a mini-review. Food Sci Appl Biotechnol 3(1):56. https://doi.org/10.30721/fsab2020.v3.i1.80

Prieto JM, Schaffner U, Barker A, Braca A, Siciliano T, Boeve J-L (2007) Sequestration of furostanol saponins by *Monophadnus* sawfly larvae. J Chem Ecol 33(3):513–524. https://doi.org/10.1007/s10886-006-9232-7

Qiu L, Zhao F, Jiang Z-H, Chen L-X, Zhao Q, Liu H-X, Yao X-S, Qiu F (2008) Steroids and flavonoids from *Physalis alkekengi* var.

franchetii and their inhibitory effects on nitric oxide production. J Nat Prod 71(4):642–646. https://doi.org/10.1021/np700713r

Ricupero M, Biondi A, Cincotta F, Condurso C, Palmeri V, Verzera A, Zappala L, Campolo O (2022) Bioactivity and physico-chemistry of garlic essential oil nanoemulsion in tomato. Entomol Gen 42(6):921–930. https://doi.org/10.1127/entomologia/2022/1553

Sakaguchi M (2020) Diverse and common features of trehalases and their contributions to microbial trehalose metabolism. Appl Microbiol Biotechnol 104(5):1837–1847. https://doi.org/10.1007/s00253-019-10339-7

Savojardo C, Martelli PL, Fariselli P, Profiti G, Casadio R (2018) BUSCA: an integrative web server to predict subcellular localization of proteins. Nucleic Acids Res 46(W1):W459-w466. https://doi.org/10.1093/nar/gky320

Sell MP, Amezian D, Heckel DG, Pauchet Y (2021) Biologicol function of solanaceous withanolides and their effexts on herbivorous insects. Annual Plant Rev Online 4(2):625–647. https://doi.org/10.1002/9781119312994.apr0779

Shukla E, Thorat LJ, Nath BB, Gaikwad SM (2015) Insect trehalase: Physiological significance and potential applications. Glycobiology 25(4):357–367. https://doi.org/10.1093/glycob/cwu125

Studer G, Rempfer C, Waterhouse AM, Gumienny R, Haas J, Schwede T (2020) QMEANDisCo-distance constraints applied on model quality estimation. Bioinformatics 36(6):1765–1771. https://doi.org/10.1093/bioinformatics/btz828

Tamura K, Stecher G, Kumar S (2021) MEGA11: molecular evolutionary genetics analysis version 11. Mol Biol Evol 38(7):3022–3027. https://doi.org/10.1093/molbev/msab120

Tan YA, Xiao LB, Zhao J, Xiao YF, Sun Y, Bai LX (2015) Ecdysone receptor isoform-B mediates soluble trehalase expression to regulate growth and development in the mirid bug, *Apolygus lucorum* (Meyer-Dur). Insect Mol Biol 24(6):611–623. https://doi.org/10.1111/imb.12185

Tang B, Wang S, Wang S-G, Wang H-J, Zhang J-Y, Cui S-Y (2018) Invertebrate trehalose-6-phosphate synthase gene: genetic architecture, biochemistry, physiological function, and potential applications. Front Physiol. https://doi.org/10.3389/fphys.2018.00030

Tang B, Wei P, Chen J, Wang S, Zhang W (2012) Progress in gene features and functions of insect trehalases. Acta Entomol Sin 55(11):1315–1321. https://doi.org/10.5555/20133040192

Tellis MB, Chaudhari BY, Deshpande SV, Nikam SV, Barvkar VT, Kotkar HM, Joshi RS (2023a) Trehalose transporter-like gene diversity and dynamics enhances stress response and recovery in *Helicoverpa armigera*. Gene. https://doi.org/10.1016/j.gene.2023.147259

Tellis MB, Kotkar HM, Joshi RS (2023b) Regulation of trehalose metabolism in insects: from genes to the metabolite window. Glycobiology 33(4):262–273. https://doi.org/10.1093/glycob/cwad011

Thorat L, Mani KP, Thangaraj P, Chatterjee S, Nath BB (2016) Down-regulation of *dTps1* in *Drosophila melanogaster* larvae confirms involvement of trehalose in redox regulation following desiccation. Cell Stress Chaperones 21(2):285–294. https://doi.org/10.1007/s12192-015-0658-0

Tissier A, Morgan JA, Dudareva N (2017) Plant volatiles: going in but not out of trichome cavities. Trends Plant Sci 22(11):930–938. https://doi.org/10.1016/j.tplants.2017.09.001

Verheggen F, Barres B, Bonafos R, Desneux N, Escobar-Gutierrez AJ, Gachet E, Laville J, Siegwart M et al (2022) Producing sugar beets without neonicotinoids: an evaluation of alternatives for the management of viruses-transmitting aphids. Entomol Gen 42(4):491–498. https://doi.org/10.1127/entomologia/2022/1511

Wan S, He J, Chao L, Shi Z, Wang S, Yu W, Huang Z, Wang S et al (2023a) Regulatory Role of Trehalose Metabolism in Cold Stress of *Harmonia axyridis* Laboratory and Overwinter Populations. Agronomy-Basel. https://doi.org/10.3390/agronomy13010148

Wan SJ, Si HR, Wang XZ, Chao L, Ma W, Sun SS, Tang B, Tan XL et al (2023b) Regulation of *Vicia faba* L. response and its effect on megoura crassicauda reproduction under zinc stress. Int J Mol Sci. https://doi.org/10.3390/ijms24119659

Wang J, Cai Q, Qiu L, Ying S, Feng M (2017a) Additive roles of two *TPS* genes in trehalose synthesis, conidiation, multiple stress responses and host infection of a fungal insect pathogen. Appl Microbiol Biotechnol 101(9):3637–3651. https://doi.org/10.1007/s00253-017-8155-2

Waterhouse A, Bertoni M, Bienert S, Studer G, Tauriello G, Gumienny R, Heer FT, de Beer TAP et al (2018) SWISS-MODEL: homology modelling of protein structures and complexes. Nucleic Acids Res 46(W1):W296-w303. https://doi.org/10.1093/nar/gky427

Weissenberg M, Levy A, Svoboda JA, Ishaaya I (1998) The effect of some Solanum steroidal alkaloids and glycoalkaloids on larvae of the red flour beetle, *Tribolium castaneum*, and the tobacco hornworm. Manduca Sexta Phytochemistry 47(2):203–209. https://doi.org/10.1016/s0031-9422(97)00565-7

Wingler A (2002) The function of trehalose biosynthesis in plants. Phytochemistry 60(5):437–440. https://doi.org/10.1016/s0031-9422(02)00137-1

Wu SJ, Ng LT, Chen CH, Lin DL, Wang SS, Lin CC (2004) Anti-hepatoma activity of *Physalis angulata P.* and *peruviana* extracts and their effects on apoptosis in human Hep G2 cells. Life Sci 74(16):2061–2073. https://doi.org/10.1016/j.lfs.2003.09.058

Wu Y, Ren D, Gao C, Li J, Du B, Wang Z, Qian S (2021) Recent advances for alkaloids as botanical pesticides for use in organic agriculture. Int J Pest Manage 69(3):288–298. https://doi.org/10.1080/09670874.2021.1917723

Xu S, Dong H, Zeng X, Zhao Z (2019) Research progress in screening and bioactivity of terpenoid botanical pesticides. Chem Indus for Prod 39(1):1–12. https://doi.org/10.5555/20193465403

Yang WJ, Chen XM, Wang SQ, Hu HX, Cheng XP, Xu LT, Ren DM, Wang XN et al (2020) 4β-Hydroxywithanolide E from Goldenberry (Whole Fruits of *Physalis peruviana* L.) as a promising agent against chronic obstructive pulmonary disease. J Nat Prod 83(4):1217–1228. https://doi.org/10.1021/acs.jnatprod.9b01265

Yu H, Huang Y, Lu Z, Zhang Q, Su H, Du Y, Yi L, Zhong B et al (2021) Inhibition of trehalase affects the trehalose and chitin metabolism pathways in *Diaphorina citri* (Hemiptera: Psyllidae). Insect Sci 28(3):718–734. https://doi.org/10.1111/1744-7917.12819

Yu L, Chen X, Wei Y, Ding Y, Wang Q, Wang S, Tang B, Wang S (2020) Effects of long-term cadmium exposure on trehalose metabolism, growth, and development of *Aedes albopictus* (Diptera: Culicidae). Ecotoxicol Environ Saf. https://doi.org/10.1016/j.ecoenv.2020.111034

Zhang B, Zhang Y, Guan R, Du M, Yin X, Zhao W, An S (2022) Trehalase is required for sex pheromone biosynthesis in Helicoverpa armigera. Insect Mol Biol 31(3):334–345. https://doi.org/10.1111/imb.12762

Zhang J, Qi L, Chen B, Li H, Hu L, Wang Q, Wang S, Xi J (2023) Trehalose-6-phosphate synthase contributes to rapid Cold hardening in the invasive insect *Lissorhoptrus oryzophilus* (Coleoptera: Curculionidae) by regulating trehalose metabolism. InSects. https://doi.org/10.3390/insects14120903

Zhang L, Qiu L-Y, Yang H-L, Wang H-J, Zhou M, Wang S-G, Tang B (2017) Study on the effect of wing bud chitin metabolism and its developmental network genes in the *Brown Planthopper Nilaparvata lugens*, by Knockdown of TRE Gene. Front Physiol. https://doi.org/10.3389/fphys.2017.00750

Zhang Y, Liu H, Zheng Z (2002) Ultrastructure of H. vigintioctomaculata and H. vigintioctopunctata. Entomological Knowl 39(2):132–135. https://doi.org/10.5555/20023069865

Zhou Y, Li X, Katsuma S, Xu Y, Shi L, Shimada T, Wang H (2019) Duplication and diversification of trehalase confers evolutionary

advantages on lepidopteran insects. Mol Ecol 28(24):5282–5298. https://doi.org/10.1111/mec.15291